FEBS Letters 581 (2007) 3027–3032

Contributions of Zn(II)-binding to the structural stability of endostatin

Qing Han, Yan Fu, Hao Zhou[1], Yingbo He, Yongzhang Luo*

Laboratory of Protein Chemistry, the Protein Science Laboratory of the Ministry of Education, Department of Biological Sciences and Biotechnology, Tsinghua University, Beijing 100084, PR China

Received 16 April 2007; revised 15 May 2007; accepted 18 May 2007

Available online 29 May 2007

Edited by Miguel De la Rosa

Abstract **Endostatin has a compact structure with a Zn(II)-binding site (His1, His3, His11, and Asp76) at the N-terminus. In this study, the effects of Zn(II)-binding on the folding and stability of recombinant human endostatin were studied. The results show that Zn(II)-binding largely stabilizes the structure of endostatin at physiological pH. Under some proteolytic conditions, Zn(II)-binding also contributes to the integrity of the N-terminus of endostatin, which is critical for endostatin to maintain a stable structure. Moreover, engineering an extra Zn(II)-binding peptide to the N-terminus of human endostatin makes this molecule more stable and cooperative in the presence of Zn(II).**

Keywords: Endostatin; Zn(II)-binding; Stability; Protein folding; Zn(II)-binding peptide

1. Introduction

Endostatin (ES), a 20 kDa C-terminal fragment of collagen XVIII, was discovered for its potent inhibitory function on angiogenesis and tumor growth without toxicity and acquired drug resistance [1–3]. X-ray crystallography of ES shows a compact structure composed of predominant β-sheets and loops, two pairs of disulfide bonds, and a Zn(II)-binding site at the N-terminus [4,5]. His1, His3, His11, and Asp76 coordinate with Zn(II) in human ES, and these four ligands are also conserved in murine and dog ES [4–6].

Among the four Zn(II)-binding ligands, His1, His3, and Asp76 are critical for Zn(II)-binding in ES [4,6]. The double mutant H1/3A, which cannot bind Zn(II), abolishes ES antitumor activity completely in the Lewis lung carcinoma model [7]. Site mutation in His11 or Asp76 also significantly reduces the antitumor activity of full length ES [7]. Recently, Javaherian and his colleagues reported that Zn(II)-binding is required for antitumor and antimigration activities of an N-terminal 27-amino-acid peptide of ES [8]. However, controversial reports on the role of Zn(II) in the biological activity of ES show that N-terminal deleted mutant of human ES act as efficiently as the wild-type ES [9–11]. In order to further explain these inconsistent results, more studies on the effects of Zn(II)-binding on ES are needed.

On the other hand, it was proposed that Zn(II) is likely to play a structural role in ES [5]. Zn(II)-dependent dimer was observed in the crystal instead of in the solution of human ES [4]. Surface plasmon resonance analysis shows that the binding of ES to heparin and heparan sulfate requires the presence of Zn(II) [12]. As an important constituent of ES, the contribution of Zn(II) to the folding behavior and the overall stability of ES has not been reported yet, nor the binding affinity between ES and Zn(II).

In this study, the effects of Zn(II)-binding on the folding and stability of recombinant human ES were studied using thermal- and guanidine hydrochloride (GdmC1)-induced unfolding monitored by differential scanning calorimetry (DSC) and tryptophan emission fluorescence, respectively. Our results show that upon Zn(II)-binding, ES is more stable against heat, denaturant, and certain proteolytic conditions. Moreover, engineering a Zn(II)-binding peptide (ZBP) to the N-terminus of ES enhances the Zn(II)-binding capacity, which endows holo ZBP-ES a more stable and cooperative structure than holo ES. These observations provide a structural basis for further understanding the molecular behavior involved in the biophysical and biological functions of ES and Zn(II).

2. Materials and methods

2.1. Preparation of ES and its variants

Both ES and ZBP-ES expressed by *Escherichia coli* were provided by Protgen Ltd. Fragment-179 was purified directly from the trypsin digested products of apo ES. Apo ES (0.5 mg/ml) was digested by 25 U/ml trypsin at 37 °C in 10 mM Tris, pH 7.4, for 20 min, then the products were applied on a SP Sepharose High Performance (Amersham) column equilibrated in 10 mM Tris–HCl, pH 8.0, and eluted by linear gradient of NaCl concentration. Protein concentrations were determined by BCA protein assay reagent kit (Pierce).

2.2. Apo and holo sample preparation and Zn(II) content analysis

To prepare the apo and holo samples, 100-fold molar excess EDTA or $ZnCl_2$ was incubated with protein sample in 5 mM Tris–HCl, pH 7.4, at room temperature overnight and then extensively dialyzed to 5 mM Tris–HCl, pH 7.4. The Zn(II) content was measured by atomic emission spectroscopy with an OPTIMA 3300RL instrument.

2.3. Determination of Zn(II)-binding affinity

The dissociation constants for Zn(II)-binding in ES and ZBP-ES were obtained from competition titration as described in Refs.

*Corresponding author. Fax: +86 10 6279 4691.
E-mail address: protein@tsinghua.edu.cn (Y. Luo).

[1]Present address: Department of Cell Biology and Physiology, Washington University Medical School, 660 S. Euclid Ave, St. Louis, MO 63110, United States.

Abbreviations: ES, endostatin; FZ, FluoZin-1, tripotassium salt; CD, circular dichroism; FPLC, fast protein liquid chromatography; GdmC1, guanidine hydrochloride; DSC, differential scanning calorimetry; ZBP, Zn(II)-binding peptide; ZBP-ES, Zn(II)-binding peptide modified endostatin

0014-5793/$32.00
doi:10.1016/j.febslet.2007.05.058

[13,14], except that Zn(II)-specific fluorescence indicator FluoZin-1 (FZ) (tripotassium salt) was used. FZ can form a 1:1 complex with Zn(II) specifically, with dramatic fluorescence intensity increase at 516 nm when excited at 495 nm [15]. FZ (0.125 μM) alone was titrated with Zn(II) to obtain the dissociation constant (K_0) of the FZ–Zn(II) complex. For determining the Zn(II)-binding affinity to ES or ZBP-ES, the mixture of FZ (0.125 μM) and ES or ZBP-ES (0.5 μM) was titrated with Zn(II). All of the experiments were carried out in 10 mM Tris–HCl, pH 7.4, at 20 °C. The following equilibria were used for calculation:

$$\frac{[\mathrm{FZ-Zn(II)}]}{[\mathrm{FZ}]_{\mathrm{total}}} = \frac{F - F_0}{F_{\max} - F_0} \quad (1)$$

$$\mathrm{FZ-Zn(II)} \overset{K_0}{\leftrightarrow} \mathrm{FZ} + \mathrm{Zn(II)} \quad K_0 = \frac{[\mathrm{FZ}][\mathrm{Zn(II)}]}{[\mathrm{FZ-Zn(II)}]} \quad (2)$$

$$\mathrm{ES-Zn(II)} \overset{K_1}{\leftrightarrow} \mathrm{ES} + \mathrm{Zn(II)} \quad K_1 = \frac{[\mathrm{ES}][\mathrm{Zn(II)}]}{[\mathrm{ES-Zn(II)}]} \quad (3)$$

$$\mathrm{ES-Zn(II)_2} \overset{K_2}{\leftrightarrow} \mathrm{ES-Zn(II)} + \mathrm{Zn(II)} \quad K_2 = \frac{[\mathrm{ES-Zn(II)}][\mathrm{Zn(II)}]}{[\mathrm{ES-Zn(II)_2}]} \quad (4)$$

where F denotes fluorescence intensity measured at the wavelength of 516 nm, F_0 is the fluorescence background of FZ, $F_{\max}$ is the maximal fluorescence intensity, K_1 and K_2 are the dissociation constants for the first and the second Zn(II) ion binding in protein, respectively. For protein which has only one Zn(II)-binding site, Eqs. (1)–(3) are used, while for protein which has two binding sites, Eqs. (1)–(4) are used. In this study K_0 = 7.87 μM was obtained, slightly deviating from the K_0 (8 μM) provided by manufacturer. Based on Zn(II) content and binding affinities of holo ES and ZBP-ES, extra Zn(II) (10-fold molar excess of protein) was added into the holo samples in the following experiments to make sure that holo ES and ZBP-ES were predominantly in the bound forms at neutral pH (>90%, according to the dissociation constants). Higher Zn(II) concentration was avoided taking account of the probability of cation or anion effect brought by $ZnCl_2$ in the unfolding studies.

2.4. Fluorescence measurements

Fluorescence measurements were carried out using an F-4500 fluorescence spectrophotometer (Hitachi) with a cuvette of 1 cm light path. The slit widths for excitation and emission were 5 and 10 nm, respectively. The scan speed was 240 nm/min [16–19].

2.5. GdmCl-induced unfolding

The concentration of ES or its variants was 0.8 μM in 5 mM Tris–HCl, pH 7.4, which contains different GdmCl concentrations ranging from 0 to 6 M. After incubation for over 120 min, fluorescence measurements were carried out. All of the measurements were repeated for three times and data were analyzed according to the procedure of Santoro and Bolen [20].

2.6. Circular dichroism (CD) spectroscopy

The far- and near-UV CD spectra were obtained using a Jasco-715 spectropolarimeter. The concentration of protein was 10 μM, in 5 mM Tris–HCl, pH 7.4. The spectra were measured in 0.1 (far-UV) and 1 cm (near-UV) quartz cuvette. An average of three scans was recorded and corrected by subtracting the baseline spectrum of the buffer. The CD signal was converted to molar ellipticity per residue [θ] (deg cm^2 dmol^{-1}). All measurements were carried out at 20 °C.

2.7. Differential scanning calorimetry (DSC)

DSC thermograms were recorded in a micro DSC III (Setaram, France). Each sample was in 10 mM HEPES buffer at pH 7.0 with a final ES concentration of 2.86 mg/ml. The heating rate is 0.5 °C/min. A reference blank containing all reagents except ES was measured for each sample at identical settings. Data were analyzed as described by Brandts and his colleagues [21].

2.8. Proteolysis assay

EDTA or $ZnCl_2$ (1 mM) was pre-incubated with ES (0.2 mg/ml) for 10 min at 37 °C before trypsin (62.5 U/ml) was added. At each time point, reaction solution was quickly taken out and mixed with reduced SDS–PAGE loading buffer to stop the proteolysis reactions. All of the experiments were carried out in PBS buffer, pH 7.4, at 37 °C.

2.9. Mass spectrometry

The largest fragment of trypsin-digested apo ZBP-ES were separated by SDS-PAGE, and then analyzed by matrix-assisted laser desorption/ionization time of flight (MALDI-TOF) mass spectrometry using a Bruker Biflex linear time-of-flight spectrometer (Bruker Franzen, Bremen, Germany). The MALDI-TOF data were searched in the Swiss-Prot protein data base for protein identification.

3. Results

3.1. Structure analyses and Zn(II)-binding affinity measurement

As described in our previous studies, tryptophan emission fluorescence is a good probe for detecting the tertiary structure changes of ES [16–19]. Fig. 1A shows a 3D structure model of ES, in which the Zn(II)-binding site and the four tryptophan residues are indicated [4]. Apo and holo ES show very similar tryptophan fluorescence spectra at neutral pH (Fig. 1B), which may imply that Zn(II)-binding has little effect on the environment in which the four tryptophan residues are located. The tertiary and secondary structure of apo and holo ES do not change much, as evidenced by the near- and far-UV CD spectra, respectively (Fig. 1C and D). These results show that Zn(II)-binding does not bring evident changes to the overall structure of ES. In our experiment, the dimer formation of holo ES was not detected in solution at physiological pH by Fast protein liquid chromatography (FPLC) size-exclusion chromatography (data not shown).

Atomic emission spectroscopy results show that holo ES contains about one Zn(II) ion per molecule (Zn(II)/ES is 0.9), which is consistent with previous reports [4,6]. The affinity of ES for Zn(II) was determined by competition titration with a Zn(II) fluorescence indicator, FluoZin-1 (FZ). Fig. 2 shows the plots of fluorescence intensity at 516 nm as a function of total added Zn^{2+}. Data of ES were best fitted to Eq. (1)–(3), which describes a single binding site for Zn^{2+}, and the dissociation constant of ES–Zn(II) complex is 6.7 nM.

3.2. Calorimetric study of ES by DSC

The thermograms showing the excess heat capacity (C_p) as a function of temperature are shown in Fig. 3. The transition temperatures (T_m) of apo ES is 52.1 °C. Zn(II)-binding shifts the transition peak towards higher temperature, with a 9.1 °C increase in ΔT_m. These results demonstrate that Zn(II)-binding stabilizes holo ES against heat.

3.3. Limited protease digestion

Trypsin is a commonly used protease, which cleaves C-terminal peptide bonds of the Arg and Lys residues. Since all of the 15 Arg and 5 Lys residues in ES are on the surface of the tertiary structure of the molecule [4], trypsin was used as a tool to probe possible conformational change of ES upon Zn(II)-binding. When digested under the same condition, apo ES was quickly digested within 10 min, while intact holo ES could not be totally digested even after 6 h (Fig. 4).

In addition, different digestion manners were observed with apo and holo ES. Apo ES experienced a two-stage digestion process, during which a dominant fragment was obtained within 3 min and was further degraded. In contrast, intact holo ES follows a continuous digestion process (Fig. 4). These results indicate that Zn(II)-binding may protect certain susceptible cleavage sites of ES thus stabilizing ES against trypsin. Peptide mass fingerprinting shows that only the first four ami-

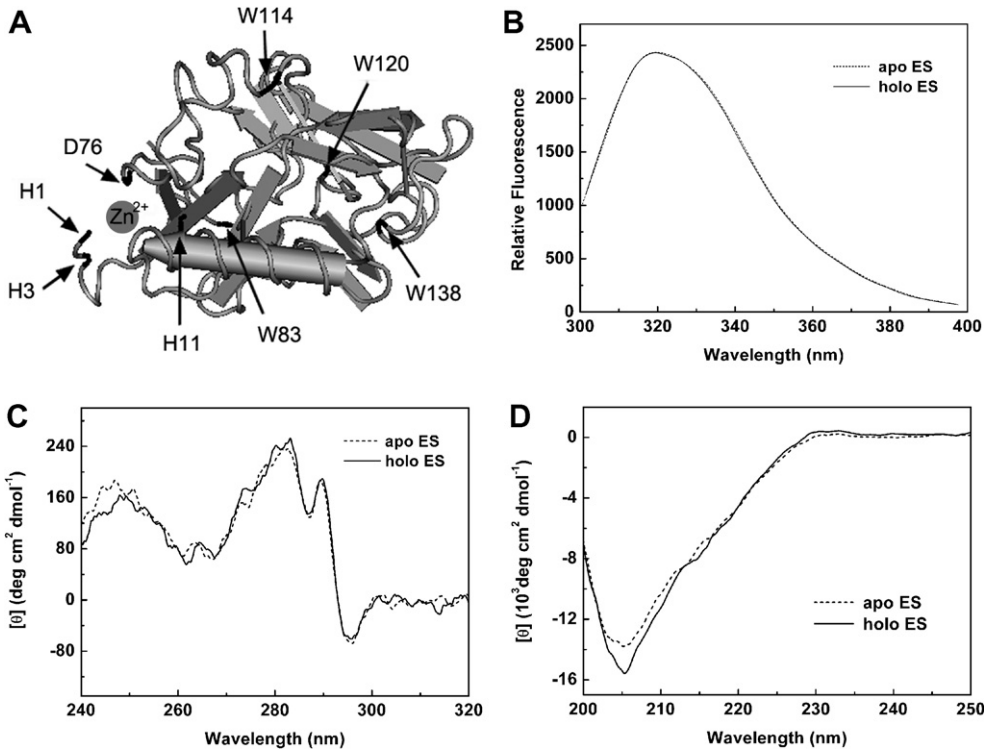

Fig. 1. Tertiary and secondary structure analyses of apo and holo ES. (A) Crystal structure diagram of ES (NCBI Chemical Data, edited by Cn3D program) [4]. (B) Fluorescence spectra excited at 288 nm. (C) Near-UV CD spectra. (D) Far-UV CD spectra. All measurements were carried out at 20 °C, and 10-fold molar excess EDTA or $ZnCl_2$ was added to apo and holo ES samples, respectively.

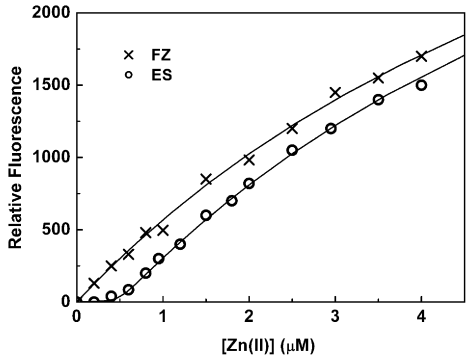

Fig. 2. Zn(II)-binding affinity measurement. Plots of fluorescence intensity at 516 nm as a function of total Zn(II) in the competition experiments using FluoZin-1 to determine the Zn(II)-binding affinity of ES. Solid lines show the fitted data.

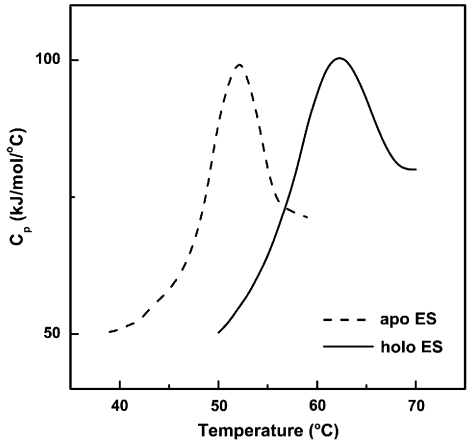

Fig. 3. DSC thermograms of apo and holo ES. All of the scans were carried out in 10 mM HEPES buffer, pH 7.0, with a heating rate of 0.5 °C/min.

no acid residues (HSHR) at the N-terminus, including two His residues from the Zn(II)-binding site, of the apo ES were lost in this main fragment. Since the N-terminal loop of ES was reported to stretch out of the core structure [4], it is reasonable to conclude that the subtle conformational change of the N-terminal loop of ES upon Zn(II)-binding may not induce an evident change to the overall structure of ES (Fig. 1B–D).

3.4. GdmCl-induced unfolding of ES

GdmCl-induced unfolding of apo and holo ES was monitored by the tryptophan emission fluorescence at 20 °C (Fig. 5A and B). The unfolding curves of holo ES has dramatic shifts towards higher GdmCl concentrations compared with apo ES, with increases in both $\Delta G^{\circ}_{\mathrm{N\text{-}U}}$ and C_{m} (Table 1). However, Zn(II)-binding causes a decrease of the m^{*} value. These results show that Zn(II)-binding largely stabilizes the structure of ES, while decreases its unfolding cooperativity.

HSHR-deficient fragment of apo ES (fragment-179) was purified from trypsin-digested products of apo ES for further study. Removal of the first four amino acid residues results in the loss of Zn(II) -binding to ES [4]. At pH 7.4, although fragment-179 shows a similar fluorescence profile as wild-type apo and holo ES (data not shown) in the absence of Zn(II), it is less stable than either apo or holo ES in GdmCl-induced

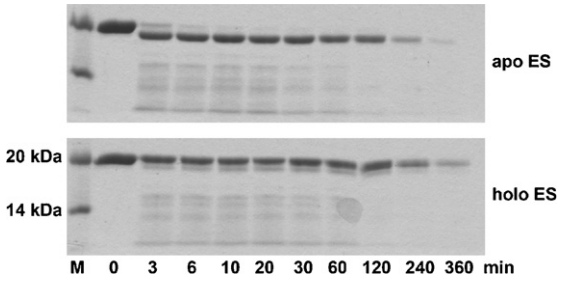

Fig. 4. Trypsin digestion profile of apo and holo ES in PBS buffer, pH 7.4, at 37 °C.

unfolding at 37 °C, at which the protease digestion was performed (Fig. 5C). The unfolding cooperativity of fragment-179 is significantly higher than that of either apo or holo ES reflected by a higher m^* (Table 1). The decreased stability together with the largely increased unfolding cooperativity implies a very fragile structure of fragment-179. In addition, the C_m of apo ES against GdmCl decreased 0.48 M when the temperature increased from 20 °C to 37 °C, while the C_m of holo ES only decreases 0.06 M (Table 1). These results show that holo ES is less sensitive to the change of temperature than apo ES during the GdmCl-induced unfolding process.

3.5. Engineering Zn(II)-binding peptide improves the biophysical properties of ES

Pharmacokinetics studies show that engineering a peptide with the sequence of MGGSHHHHH at the N-terminus of human ES endows ES a much longer half life at equal dose in animal models [22,23]. Since this engineered sequence contains five His residues in a row, which might serve as a Zn(II)-binding peptide (ZBP), it is reasonable to hypothesize that this ZBP upon binding to Zn(II) may contribute to the improved pharmacokinetics properties. Indeed, ZBP-ES was measured to bind one more Zn(II) ion than ES in solution in our study. Using two Zn(II)-binding sites model in the competition titration, the first (K_1) and the second (K_2) dissociation constant for ZBP-ES were measured to be 9 nM and 44.7 nM, respectively. Taking account of the K_1 of ES, the K_1 of ZBP-ES may be responsible for the intrinsic Zn(II)-binding site (composed by His1, His3, His11, and Asp76), and K_2 is for ZBP.

GdmCl-induced unfolding of ZBP-ES shows that Zn(II)-binding also largely stabilizes ZBP-ES (Fig. 6). From the parameters listed in Table 1, upon Zn(II)-binding, the $\Delta G^{\circ}_{N\text{-}U}$, m^*, and C_m of holo ZBP-ES increase more dramatically than those of holo ES, which results higher stability and cooperativity of holo ZBP-ES than holo ES. ES mutant D76A was reported to have no Zn(II)-binding ability [6]. To exclude the possible structural role of the ZBP itself, we used mutant ZBP-ES-D76A to study the GdmCl-induced unfolding. Results show that holo ZBP-ES-D76A can bind one Zn(II), however, Zn(II)-binding cannot stabilize holo ZBP-ES-D76A (Table 1). These results demonstrate that the two Zn(II) ions in ZBP-ES have a synergetic effect on the structural stability and unfolding cooperativity of ZBP-ES. It is also quite possible that in ZBP-ES or ZBP-ES-D76A the coordination pattern is rearranged using the possible Zn(II) ligands such as Asp5 which was found to be another Zn(II)-binding ligand in murine ES under certain conditions [6].

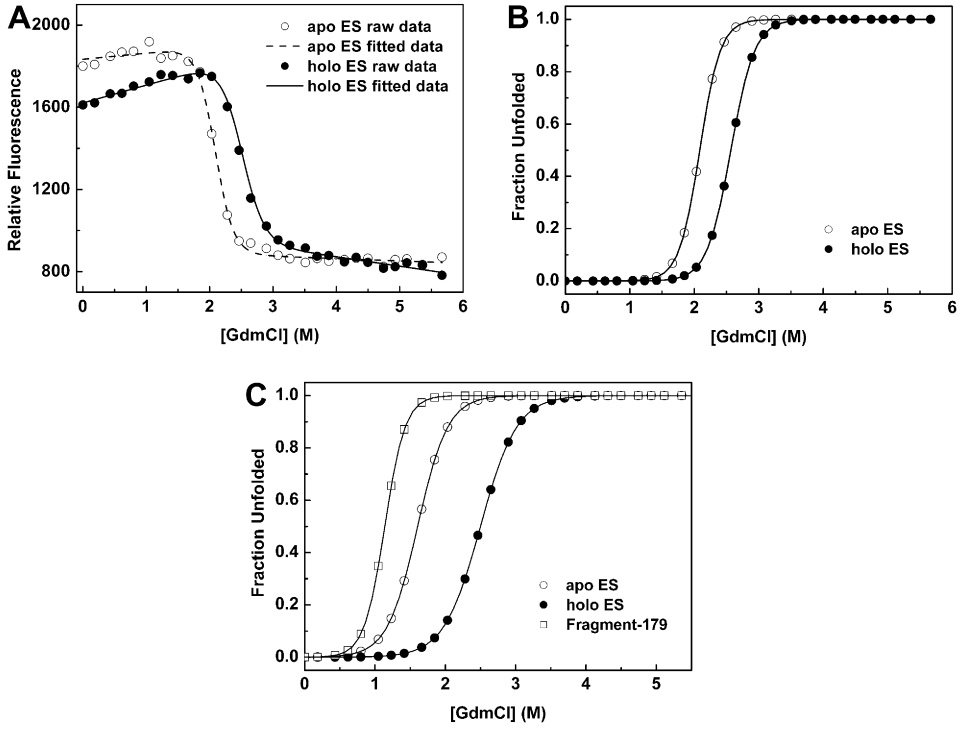

Fig. 5. GdmCl-induced unfolding of ES monitored by the tryptophan emission fluorescence. (A) Raw data and fitted data of unfolding process of ES using relative fluorescence intensity monitored at 318 nm at 20 °C. (B) Normalized data of A. (C) Normalized data of GdmCl-induced unfolding of ES and purified fragment-179 at 37 °C.

Table 1
Parameters of GdmCl-induced unfolding

	$\Delta G^{\circ}_{N\text{-}U}$ [a] (kJ mol^{-1})	m^{*} [b] (kJ mol^{-1} M^{-1})	C_m [c] (M)
Apo ES, 20 °C	30.47	14.58	2.09
Holo ES, 20 °C	33.89	13.24	2.56
Apo ES, 37 °C	18.58	11.54	1.61
Holo ES, 37 °C	23.95	9.58	2.50
Fragment-179, 37 °C	19.37	16.99	1.14
Apo ZBP-ES, 20 °C	24.84	12.06	2.06
Holo ZBP-ES, 20 °C	40.84	15.47	2.64
Apo ZBP-ES-D76A, 20 °C	21.41	11.96	1.79
Holo ZBP-ES-D76A, 20 °C	11.78	6.58	1.79

[a] $\Delta G^{0}_{N\text{-}U}$, the free energy change in the absence of denaturant.
[b] m^{*}, the apparent m value defined by the linear extrapolation model.
[c] C_m, the concentration of GdmCl at the midpoint of the unfolding transition.

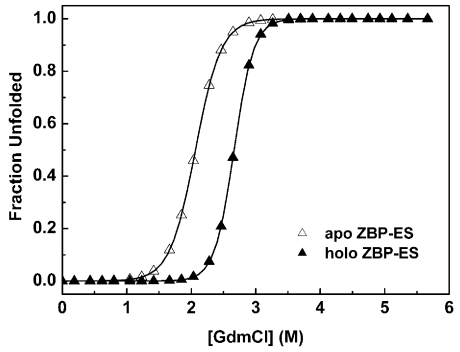

Fig. 6. GdmCl-induced unfolding of apo and holo ZBP-ES. The symbols are normalized data. All of the measurements were carried out at 20 °C.

4. Discussion

Our group previously reported that ES is acid-resistant, and its two pairs of disulfide bonds contribute significantly to the structural stability and the biological activity of ES [16–19]. Here, we show that Zn(II) is another important factor to the stability of ES, which provides clues to the refolding, preparation, and preservation of ES. It is also very necessary to distinguish the apo and holo forms in future studies on biophysical and biochemical properties of ES. These results also provide insight into the function of Zn(II) on ES activity, which may partly take effect through stabilizing the N-terminus of ES, and thus stabilize the entire tertiary structure.

Holo ES, which is speculated to be dominant in vivo [4], shows higher stability than apo ES. It is reasonable to hypothesize that Zn(II)-binding enables holo ES to be more resistant under stressed conditions and retain a higher stability in circulation than apo ES. Fragment-179 is one species existing in the recombinant human ES products expressed by *Pichia pastoris* [22]. Our studies on the decreased stability of fragment-179 may provide an explanation for the short half lives of ES in some pharmacokinetics studies, in which ES expressed by *P. pastoris* was used [22].

It has been reported that ZBP-ES has an anti-tumor activity with high clinical benefit rate and is well tolerated in pretreated advanced non-small cell lung cancer patients [24,25]. Compared with ES, the therapeutic doses of ZBP-ES are lower and the half lives at equal doses are longer in both animal tests and clinical studies [22–27]. These observations may imply the higher efficacy and stability of ZBP-ES in vivo. Parallel studies show that ZBP-ES has more potent anti-angiogenic activities in vitro and anti-tumor activities in vivo compared with ES (to be submitted). From our studies on the structural roles of Zn(II)-binding in ES and ZBP-ES, a plausible explanation of the above phenomena is that the stable structure of holo ZBP-ES lowers its clearance rate from the body.

Acknowledgement: This work was supported by grants from the Major Program of National Science Foundation of China (No. 30291000). We gratefully acknowledge members of the Luo laboratory for insightful discussions and criticism throughout the course of this work.

References

[1] O'Reilly, M.S., Boehm, T., Shing, Y., Fukai, N., Vasios, G., Lane, W.S., Flynn, E., Birkhead, J.R., Olsen, B.R. and Folkman, J. (1997) Endostatin: an endogenous inhibitor of angiogenesis and tumor growth. Cell 88, 277–285.
[2] Sasaki, T., Fukai, N., Mann, K., GoÈhring, W., Olsen, B.R. and Timpl, R. (1998) Structure, function and tissue forms of the C-terminal globular domain of collagen XVIII containing the angiogenesis inhibitor endostatin. EMBO J. 17, 4249–4256.
[3] Boehm, T., Folkman, J., Browder, T. and O'Reilly, M.S. (1997) Antiangiogenic therapy of experimental cancer does not induce acquired drug resistance. Nature 390, 404–407.
[4] Ding, Y.H., Javaherian, K., Lo, K.M., Chopra, R., Boehm, T., Lanciotti, J., Harris, B.A., Li, Y., Shapiro, R., Hohenester, E., Timpl, R., Folkman, J. and Wiley, D.C. (1998) Zinc-dependent dimers observed in crystals of human endostatin. Proc. Natl. Acad. Sci. USA 95, 10443–10448.
[5] Hohenester, E., Sasaki, T., Olsen, B.R. and Timpl, R. (1998) Crystal structure of the angiogenesis inhibitor endostatin at 1.5 Å resolution. EMBO J. 17, 1656–1664.
[6] Hohenester, E., Sasaki, T., Meann, K. and Timpl, R. (2000) Variable zinc coordination in endostatin. J. Mol. Biol. 297, 1–6.
[7] Boehm, T., O'Reilly, M.S., Keough, K., Shiloach, J., Shapiro, R. and Folkman, J. (1998) Zinc-binding of endostatin is essential for its antiangiogenic activity. Biochem. Biophys. Res. Commun. 252, 190–194.
[8] Tjin Tham Sjin, R.M., Satchi-Fainaro, R., Birsner, A.E., Ramanujam, V.M., Folkman, J. and Javaherian, K. (2005) A 27-amino-acid synthetic peptide corresponding to the NH2-terminal zinc-binding domain of endostatin is responsible for its antitumor activity. Cancer Res. 65, 3656–3663.
[9] Yamaguchi, N., Anand-Apte, B., Lee, M., Sasaki, T., Fukai, N., Shapiro, R., Que, I., Lowik, C., Timpl, R. and Olsen, B.R. (1999) Endostatin inhibits VEGF-induced endothelial cell migration and tumor growth independently of zinc-binding. EMBO J. 18, 4414–4423.
[10] Chillemi, F. and Francescato, P. (2003) Studies on the structure–activity relationship of endostatin: synthesis of human endostatin peptides exhibiting potent antiangiogenic activities. J. Med. Chem. 46, 4165–4172.
[11] Cho, H.Y., Kim, W.J., Lee, Y.M., Kim, Y.M., Kwon, Y.G., Park, Y.S., Choi, E.Y. and Kim, K.W. (2004) N-/C-terminal deleted mutant of human endostatin efficiently acts as an anti-angiogenic and anti-tumorigenic agent. Oncol. Rep. 11, 191–195.
[12] Ricard-Blum, S., Feraud, O., Lortat-Jacob, H., Rencurosi, A., Fukai, N., Dkhissi, F., Vittet, D., Imberty, A., Olsen, B.R. and van der Rest, M. (2004) Characterization of endostatin binding to heparin and heparan sulfate by surface plasmon resonance and molecular modeling – role of divalent cations. J. Biol. Chem. 279, 2927–2936.
[13] de Seny, D., Heinz, U., Wommer, S., Kiefer, M., Meyer-Klaucke, W., Galleni, M., Frere, JM., Bauer, R. and Adolph, H.W. (2001) Metal ion binding and coordination geometry for wild type and mutants of metallo-beta-lactamase from Bacillus cereus 569/H/9

(Bell): a combined thermodynamic, kinetic, and spectroscopic approach. J. Biol. Chem. 276, 45065–45078.
[14] Liu, J., Stemmler, A.J., Fatima, J. and Mitra, B. (2005) Metal-binding characteristics of the amino-terminal domain of ZntA: binding of lead is different compared to cadmium and zinc. Biochemistry 44, 5159–5167.
[15] Gee, K.R., Zhou, Z.-L., Ton-That, D., Sensi, S.L. and Weiss, J.H. (2002) Measuring zinc in living cells. A new generation of sensitive and selective fluorescent probes. Cell Calcium 31, 245.
[16] Li, B., Wu, X., Zhou, H., Chen, Q. and Luo, Y. (2004) Acid-induced unfolding mechanism of recombinant human endostatin. Biochemistry 43, 2550–2557.
[17] Wu, X., Huang, J., Chang, G. and Luo, Y. (2004) Detection and characterization of an acid-induced folding intermediate of endostatin. Biochem. Biophys. Res. Commun. 320, 973–978.
[18] Zhou, H., Wang, W. and Luo, Y. (2005) Contributions of disulfide bonds in a nested pattern to the structure, stability, and biological functions of endostatin. J. Biol. Chem. 280, 11303–11312.
[19] He, Y., Zhou, H., Tang, H. and Luo, Y. (2006) Deficiency of disulfide bonds facilitating fibrillogenesis of endostatin. J. Biol. Chem. 281, 1048–1057.
[20] Santoro, M.M. and Bolen, D.W. (1988) Unfolding free energy changes determined by the linear extrapolation method. 1. Unfolding of phenylmethanesulfonyl alpha-chymotrypsin using different denaturants. Biochemistry 27, 8063–8068.
[21] Brandts, J.F., Hu, C.Q. and Lin, L. (1989) A simple model for proteins with interacting domains: applications to scanning calorimetry data. Biochemistry 28, 8588–8596.
[22] Sim, B.K., Fogler, WE., Zhou, X.H., Liang, H., Madsen, J.W., Luu, K., O'Reilly, M.S., Tomaszewski, I.E. and Fortier, A.H. (1999) Zinc ligand-disrupted recombinant human endostatin: potent inhibition of tumor growth, safety and pharmacokinetic profile. Angiogenesis 3, 41–51.
[23] Song, H.F., Liu, X.W., Zhang, H.N., Zhu, B.Z., Yuan, S.J., Liu, S.Y. and Tang, Z.M. (2005) Pharmacokinetics of His-tag recombinant human endostatin in Rhesus monkeys. Acta Pharmacol. Sin. 26, 124–128.
[24] Yang, L., Wang, J.W., Tang, Z.M., Liu, X.W., Huang, J., Li, S.T., Dong, Y., Zhang, H.P., Xue, L., Chu, D.T. and Sun, Y. (2004) A Phase I clinical trial for recombinant human endostatin. Chin. J. New Drugs 13, 548–553.
[25] Yang, L., Wang, J.W., Sun, Y., Zhu, Y.Z., Liu, X.Q., Li, W.L., Di, L.J., Li, P.W., Wang, Y.L., Song, S.P., Yao, C. and You, L.F. (2006) Randomized phase II trial on escalated doses of Rh-endostatin (YH-16) for advanced non-small cell lung cancer. Zhonghua Zhong Liu Za Zhi 28, 138–141, (in Chinese).
[26] Hansma, A.H., Broxterman, H.J., van der Horst, I., Yuana, Y., Boven, E., Giaccone, G., Pinedo, H.M. and Hoekman, K. (2005) Recombinant human endostatin administered as a 28-day continuous intravenous infusion, followed by daily subcutaneous injections: a phase I and pharmacokinetic study in patients with advanced cancer. Ann. Oncol. 16, 1695–1701.
[27] Thomas, J.P., Arzoomanian, R.Z., Alberti, D., Marnocha, R., Lee, R., Friedl, A., Tutsch, K., Dresen, A., Geiger, P., Pluda, J., Fogler, W., Schiller, J.H. and Wilding, G. (2003) Phase I pharmacokinetic and pharmacodynamic study of recombinant human endostatin in patients with advanced solid tumors. J. Clin. Oncol. 21, 223–231.